Measurement of 10-fs Laser Pulses

Greg Taft, Andy Rundquist, Margaret M. Murnane, *Member, IEEE*, Ivan P. Christov, Henry C. Kapteyn, Kenneth W. DeLong, David N. Fittinghoff, Marco A. Krumbügel, John N. Sweetser, and Rick Trebino

(Invited Paper)

***Abstract*—We report full characterization of the intensity and phase of ∼10-fs optical pulses using second-harmonic-generation frequency-resolved-optical-gating (SHG FROG). We summarize the subtleties in such measurements, compare these measurements with predicted pulse shapes, and describe the implications of these measurements for the creation of even shorter pulses. We also discuss the problem of *validating* these measurements. Previous measurements of such short pulses using techniques such as autocorrelation have been difficult to validate because at best incomplete information is obtained and internal self-consistency checks are lacking. FROG measurements of these pulses, in contrast, *can* be validated, for several reasons. First, the complete pulse-shape information provided by FROG allows significantly better comparison of experimental data with theoretical models than do measurements of the autocorrelation trace of a pulse. Second, there exist internal self-consistency checks in FROG that are not present in other pulse-measurement techniques. Indeed, we show how to *correct* a FROG trace with systematic error using one of these checks.**

I. Introduction

THE GENERATION of ultrashort laser pulses with durations on the order of 10 fs is now routine [1]–[4]. But, while pulse generation in this extremely short-pulse regime is well studied, pulse *measurement* in this regime, while commonly performed, has not received a great deal of study. It is generally assumed that autocorrelation and interferometric-autocorrelation measurements of such short pulses are accurate, but this assumption has never, to our knowledge, been carefully checked. One reason for this, we believe, is that autocorrelation measurements do not yield full pulse characterization, so that ambiguity is necessarily already present in the measurement. Another reason is undoubtedly that it is also quite difficult to check these measurements, because no internal consistency checks exist for autocorrelation, except for the not-particularly-restrictive requirements that the trace be symmetric and the pulse time-bandwidth product be greater than the theoretical limit for the assumed pulse shape [5]. Finally, considerable effort has been devoted to comparing autocorrelation traces with those for pulses predicted by theoretical models, but the unavoidable ambiguities that necessarily accompany autocorrelation measurements severely limit the utility of such comparisons. Clearly, a means of accurately measuring the full pulse shape would provide a better check of theoretical models and, simultaneously, a better check of the pulse measurement itself.

In this paper, we attempt to improve this situation by describing second-harmonic-generation frequency-resolved-optical-gating (SHG FROG) [6]–[11] measurements of ∼10-fs pulses from a Ti:Sapphire laser. These measurements address all of the above issues. First, FROG yields the full intensity and phase of ultrashort pulses. No ambiguity exists in our pulse measurements (we remove the direction-of-time ambiguity usually present in SHG FROG measurements). Second, unlike autocorrelation techniques, FROG contains internal consistency checks, which can be performed on the measured trace and retrieved pulse, virtually guaranteeing the validity of the data. These take the form of "marginals" of the trace, that is, integrals of the trace with respect to one of its variables. For example, the frequency marginal, obtained by integrating the SHG FROG trace with respect to delay, has been shown to be equal to the autoconvolution of the pulse spectrum [8], [11]. Thus, an independent measurement of the pulse spectrum can then corroborate the measured FROG trace. It is a particularly convincing check because the two measurements occur at very different wavelengths, one at the fundamental and the other at the second harmonic, and systematic error that may be present in one wavelength range is unlikely to also be present at the other. Finally, to further validate these measurements, we also compare the full-measured pulse intensity and phase with pulse shapes predicted by theoretical models of pulse-generation in the laser [3], [12]–[14].

We also discuss the experimental issues associated with the measurement of some of the shortest pulses created. An SHG FROG device is simply a (noncollinear) autocorrelator followed by a spectrometer. While spectrally resolving and then detecting broad-band light is not excessively difficult, it must be done with wavelength-independent sensitivity or at least with known wavelength-dependent sensitivity that can be numerically compensated afterward. With numerous optical elements present, this can be more complex than first imagined. Nevertheless, most of the experimental factors that can effect the validity of the measurement lie within the autocorrelator apparatus. In particular, we find that simple autocorrelation measurements of such extremely short pulses

Manuscript received October 18, 1996; revised January 10, 1997. The work of G. Taft, A. Rundquist, M. M. Murnane, I. P. Christov, and H. C. Kapteyn was supported by the National Science Foundation. The work of K. W. DeLong, D. N. Fittinghoff, M. A. Krumbügel, J. N. Sweetser, and R. Trebino was supported by the Department of Energy, Basic Energy Sciences, Chemical Sciences Division, and the Alexander von Humboldt Foundation.

G. Taft, A. Rundquist, M. M. Murnane, I. P. Christov, and H. C. Kapteyn are with Center for Ultrafast Optical Science, University of Michigan, Ann Arbor, MI 48109 USA.

K. W. DeLong, D. N. Fittinghoff, M. A. Krumbügel, J. N. Sweetser, and R. Trebino are with the Combustion Research Facility, Sandia National Laboratories Livermore, CA 94550 USA.

Publisher Item Identifier S 1077-260X(96)09672-4.

1077–260X/96$5.00 © 1996 IEEE

also involve difficulties resulting from the large bandwidths involved. Pulses with FWHM bandwidths of 170 nm or more can easily be generated from self-modelocked Ti : Sapphire lasers. Not only must the entire spectrum of these pulses reach the frequency-conversion crystal without phase distortions, but it also must undergo frequency conversion with minimal variation in detection efficiency due to phase-matching. This necessitates the use of reflective (not refractive) optics, an extremely thin frequency-doubling crystal, and a small-angle beam geometry that minimizes geometrical smearing of the trace due to simultaneous sampling of a range of delays. It is an arduous task to verify that artifacts from these effects do not affect an autocorrelation trace. We discuss these problems for both autocorrelation and FROG. Aided by the consistency checks inherent in FROG, we have been able to overcome these experimental difficulties and achieve a high degree of confidence in our measurements. Indeed, using these consistency checks, we can even *correct* a FROG trace made using a SHG crystal with too little bandwidth or with optics or a detector with wavelength-dependent reflectivity or transmission. This correction can even be done when the error due to these effects is unknown.

It is worth mentioning that the above issues are a subset of those important in *interferometric* autocorrelation, in which the required interferometer carries with it numerous additional experimental issues. Users of interferometric autocorrelation are quite familiar with the sensitivity of the measured interferometric autocorrelation trace to alignment parameters, and the role of potential alignment-induced artifacts in this technique has never, to our knowledge, been addressed. We do not consider these issues here because, although an "interferometric FROG" technique will likely be useful for sub-5-fs pulses, FROG so far has not used an interferometric autocorrelator and hence obviously avoids these problems. Finally, interferometric autocorrelation also lacks internal consistency checks beyond the simple symmetry requirement common to noninterferometric autocorrelation.

Previous studies of the pulse-measurement process have not specifically dealt with this extremely short time scale (although some continue to apply here) and instead have dealt mainly with artifacts in noncollinear autocorrelation. Weiner [15] treated the problem of autocorrelation using a crystal with too little bandwidth. He found that the autocorrelation trace could increase or decrease in width as a result of this effect, depending on the pulse shape. Fischer and Rempel [16] studied this effect for some specific pulse shapes. Other work in this area includes that of Sala *et al.* [5], who considered higher order autocorrelations and Mindl *et al.* [17], who studied the effect of a quasicontinuous background in interferometric autocorrelation.

In Section II, we summarize the SHG FROG technique. In Section III, we discuss some of the above experimental issues that occur in measuring ultrashort pulses, including phase-matching bandwidth, detector response, and the potential geometrical distortions resulting from the use of a nonzero beam angle. For the latter effect, we derive an analytical expression for the error in the measured pulse width due to this effect and show that it is small for our measurements. We show how to use FROG's internal consistency checks to verify the validity of the measured trace. We also show how to correct a trace for frequency-dependent systematic error. In Section IV, we describe our SHG FROG apparatus, and in Section V, we present the experimental measurements of pulse intensity and phase for ~10-fs pulses. We used a thin film nonlinear medium with sufficient phase-matching bandwidth to measure a 13-fs near-transform-limited pulse. Using FROG's internal consistency checks, we show that this measurement represents an accurate determination of the pulse. We further confirm this conclusion by remeasuring the pulse after propagation through a 1-mm window and comparing the two measurements using the known dispersion of the window—a type of check possible only when the full intensity and phase of the pulse are measured. We also used a bulk KDP crystal with *insufficient* bandwidth to measure a 12-fs pulse with a double-peaked spectrum. Then, using FROG's internal consistency checks, we actually correct this FROG trace for this, as well as other, potentially unknown, systematic errors. We then compare the retrieved pulse shape with theoretical models of pulse generation in femtosecond lasers (Section VI).

II. SHG FROG

While third-order nonlinear-optical processes have been used in FROG devices to uniquely measure ultrashort laser pulses, we chose the technique of SHG FROG for this work because it is the most sensitive FROG geometry. The pulse energy available directly from a Ti : Sapphire laser, at less than 5 nJ, is too weak for current third-order FROG methods.

The electric field of a light pulse (regardless of duration) can be represented by:

$$E(t) = \mathrm{Re}\left\{\sqrt{I(t)}\,\exp\left[-i\omega_0 t - i\varphi(t)\right]\right\} \tag{1}$$

where $I(t)$ and $\varphi(t)$ are the time-dependent intensity and phase of the pulse, and ω_0 is the carrier frequency. In the frequency domain, the field can be written as

$$\tilde{E}(\omega) = \sqrt{\tilde{I}(\omega-\omega_0)}\,\exp\left[i\tilde{\varphi}(\omega-\omega_0)\right] \tag{2}$$

where $\tilde{E}(\omega)$ is simply the Fourier transform of $E(t)$, and we have neglected the negative-frequency component of $\tilde{E}(\omega)$. $\tilde{I}(\omega-\omega_0)$ is the spectral intensity, and $\tilde{\varphi}(\omega-\omega_0)$ is the spectral phase.

FROG operates in the "time-frequency domain," using measurements with simultaneous temporal and spectral resolution. It yields the full intensity and phase in either domain (and hence both domains). Specifically, FROG involves spectrally resolving the signal pulse in an autocorrelation measurement, and plotting the signal spectrum versus delay, instead of the signal energy versus delay. This yields a spectrogram of the pulse. In SHG FROG, the signal beam from an SHG autocorrelator is spectrally resolved. In the case of ideal SHG the result corresponds to

$$I_{\mathrm{FROG}}^{\mathrm{SHG}}(\omega,\tau) = \left|\int_{-\infty}^{\infty} E(t)\,E(t-\tau)\,\exp\left(-i\omega t\right)dt\right|^2. \tag{3}$$

An iterative deconvolution algorithm extracts the pulse intensity and phase from the FROG trace by finding the electric field that best reproduces the trace. Extensive numerical testing has proven the robustness of the algorithm in its ability to uniquely converge for test and experimental pulses. Since SHG FROG has been discussed in detail in previous work [7], [8], [10], [11], [18], we omit further discussion of the deconvolution algorithm and the SHG FROG trace, except to mention that, unlike other versions of FROG, the SHG FROG trace is symmetrical with respect to delay and hence has ambiguity in the direction of time. In other words, $E(t)$ and $E(-t)$ yield identical SHG FROG traces (that is, $\mathcal{E}(t)$ and $\mathcal{E}^*(-t)$, if $\mathcal{E}$ is the complex amplitude of the pulse), and thus cannot be distinguished in a single SHG FROG trace. This is, however, not usually a problem because it is usually the case that one knows in advance something about the pulse that resolves this ambiguity. For example, the pulse is often known *a priori* to be positively chirped, thus distinguishing it from its time-reversed replica, which is negatively chirped. In addition, the ambiguity may be removed by making a second SHG FROG trace after chirping the pulse somewhat with a thick piece of glass. The two resulting pulses are consistent with only one direction of time. Finally, we have found that allowing the pulse to first propagate through a thin, uncoated piece of glass, whose surface reflections add a small trailing satellite pulse a known time after the pulse, easily distinguish the pulse from its time-reversed version, which has a leading satellite pulse. The direction-of-time ambiguity thus can be simply and conclusively eliminated in SHG FROG measurements.

III. Experimental Issues and Consistency Checks

Because ~10-fs near-IR pulses have very large bandwidths of 100 nm or more, the finite phase-matching bandwidth of the autocorrelator SHG crystal may be insufficient, resulting in distortions in the signal spectrum. Because the ordinary and extraordinary refractive indices of the crystal vary with wavelength independently, an SHG crystal that is phase-matched for its central frequency will not convert all spectral components of the pulse with equal efficiency. The mathematical expression for the frequency-dependent conversion efficiency due to phase mismatch is [15]:

$$F(2\omega) = \frac{\sin^2\left[\dfrac{\Delta k(2\omega)L}{2}\right]}{\left[\dfrac{\Delta k(2\omega)L}{2}\right]^2} \tag{4}$$

where 2ω is the angular frequency of the second-harmonic light, $\Delta k(2\omega) = (2\omega/c)\left[n_e(2\omega, \theta) - n_o(\omega)\right]$ for type-I phase-matching, n_e and n_o are the extraordinary and ordinary indices of refraction, θ is the phase matching angle of the crystal, c is the speed of light in a vacuum, and L is the crystal thickness. For an accurate pulse measurement (in FROG *and* autocorrelation), one must convert not only the spectral components within this peak, but also the spectral components in the wings of the spectrum. Proper orientation of the crystal allows $n_e(2\omega, \theta) - n_o(\omega)$ to vanish for the center frequency of the pulse, and the thinner the crystal the broader the frequency range over which conversion efficiency is strong (and hence wavelength independent).

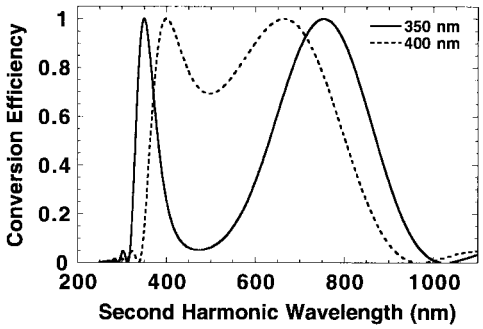

Fig. 1. Calculated second-harmonic conversion efficiency for a thin (60 μm) KDP crystal oriented for maximum conversion to 350 nm (solid curve) and 400 nm (dashed curve). The double-peaked nature of these curves occurs because two disparate wavelengths are phase-matched for a given crystal orientation, and, for a thin enough crystal, the two regions can overlap. Nevertheless, variations in the phase-matching efficiency will occur over the bandwidth of a ~100-nm pulse.

Fig. 1 shows the calculated conversion efficiency versus wavelength for a KDP crystal with a thickness of 60 μm. The solid and dashed curves assume that the crystal is oriented so that it is phase-matched to frequency-double 700- and 800-nm fundamental light, respectively. The unintuitive, non-sinc^2, variations in these efficiency curves occur because, for a given crystal angle, two different wavelengths achieve perfect phase-matching. And for a sufficiently thin crystal, these regions can overlap. While this overlap can increase the overall crystal phase-matching bandwidth, it will never yield a flat efficiency curve, the desired result for pulse measurement. In addition, due to the asymmetry in the phase-matching curve, the orientation of the crystal that gives the most intense second-harmonic light can be different from the orientation that gives the flattest conversion efficiency across the broadest spectral bandwidth. Experimentally, we have found this to be the case. In any case, it is clear that, for a pulse with a ~100-nm bandwidth (and hence with second-harmonic bandwidth ~35 nm), some variation in efficiency will occur over the pulse bandwidth. In principle, correction for this efficiency variation in the phase-matching curve is possible if one knows the specific angles and wavelengths used and the precise refractive indices of the crystal. Unfortunately, in practice, this type of correction is difficult because the precise phase-matching efficiency curve depends quite sensitively on these parameters and is difficult to know for a given measurement. As a result, such correction is impractical, if not impossible. Fortunately, we will show that such correction (as well as correction for other effects) can be done fairly easily in FROG *after the fact* and without the need to know any of the various parameters using one of FROG's internal-consistency checks.

Alternatively, an even thinner SHG crystal could in theory completely solve the finite-phase-matching bandwidth problem and obviate the need for sensitive angle tuning. Unfortunately, with the use of such thin crystals, the second-harmonic signal

levels can become too low for characterizing very low-energy pulses. Fortunately, the recent development of poled polymer films with high-second-order nonlinear coefficients can efficiently and accurately frequency-double ultrashort nanojoule pulses. Because these films can have a thickness of less than 1 μm, phase-matching is assured for all frequencies for even the shortest pulses [19]. Unfortunately, absorption in these films can also distort the SHG efficiency versus wavelength and hence may limit their usefulness with pulses significantly less than 10 fs, although this can also be corrected. In Section V, we describe a measurement we performed that shows that such a film can be used for measuring 13-fs pulses with no difficulties.

As mentioned above, FROG provides consistency checks not available with autocorrelation measurements. These checks allow us, for example, to ensure that the entire pulse spectrum is being converted to second-harmonic light. This is accomplished by comparing the "frequency marginal" of the FROG trace with the independently measured pulse spectrum. The frequency marginal is the FROG trace integrated with respect to the delay variable [8], [11]:

$$M_{\mathrm{FROG}}^{\mathrm{SHG}}(\omega) \equiv \int_{-\infty}^{\infty} I_{\mathrm{FROG}}^{\mathrm{SHG}}(\omega, \tau)\, d\tau. \tag{5}$$

It can be shown to be equal to the autoconvolution of the fundamental pulse spectrum:

$$M_{\mathrm{FROG}}^{\mathrm{SHG}}(\omega - 2\omega_0) = \tilde{I}(\omega - \omega_0) * \tilde{I}(\omega - \omega_0). \tag{6}$$

In this manner, the FROG trace may be checked against the relatively easily measured spectrum. There is also a delay marginal, which can be compared with the autocorrelation, and as a result is less useful here. The marginals of FROG traces were discussed in detail in previous publications [8], [11].

We have found the frequency-marginal comparison to be extremely useful in checking for sufficient phase-matching bandwidth, crystal-angle orientation, and for proper calibration of the varying spectral response of our spectrometer and CCD detector. Fig. 2 shows an example of how the frequency marginal can be used to optimize the SHG phase-matching angle. Initially, when the frequency marginal (open circles in Fig. 2) of a 13-fs pulse was compared to the autoconvolution (solid line) of the fundamental spectrum, there was a slight discrepancy. After a small adjustment of the phase-matching angle (less than 2°), significantly better agreement was obtained (solid squares). The frequency-marginal test is also useful in testing the nonlinear SHG films described above and in [19]. The open circles in Fig. 3 show the frequency marginal of a 13-fs pulse's FROG trace generated with a thin (0.4-μm thick) nonlinear poled polymer film of tricyanovinylaniline (PhTCV). The good agreement with the autoconvolution of the fundamental spectrum (solid line in Fig. 3) shows that the film was able to convert the entire spectrum of this 13-fs pulse to the second harmonic without variation in efficiency over the entire bandwidth of the pulse. These measurements are described in greater detail in [19].

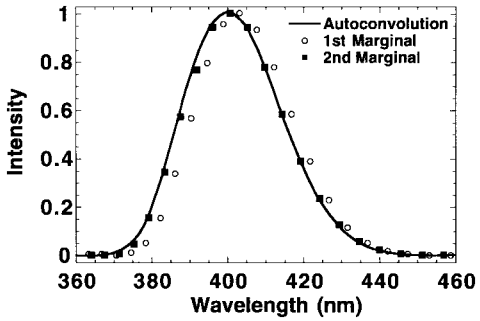

Fig. 2. Autoconvolution (solid line) of a 90 nm bandwidth spectrum compared to two FROG frequency marginals (squares and circles). The better agreement of the second frequency marginal (solid squares) was obtained after slight adjustment of the phase-matching angle.

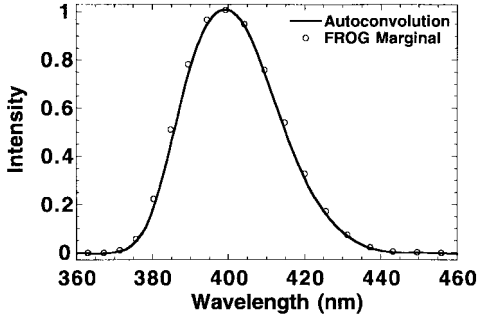

Fig. 3. Autoconvolution (solid line) of a 90-nm-bandwidth spectrum compared to the frequency marginal (circles) of a FROG trace generated using a thin (0.4-μm thick) nonlinear poled polymer film of tricyanovinylaniline (PhTCV).

It is also important to note that, in general, for broad-bandwidths corresponding to sub-20-fs pulses, the spectral response of gratings or CCD detectors cannot be assumed to be flat across the entire bandwidth of the pulse. Thus, calibration of the spectral response is required, and the frequency marginal test is a very useful (and necessary) check on the integrity of the data. Such a check—which is especially useful because the two measurements to be compared occur at very different wavelengths, the fundamental and the second harmonic—is not possible in autocorrelation or interferometric autocorrelation.

Indeed, knowing the autoconvolution of the pulse spectrum, one can *correct* the FROG trace for all of the above frequency-dependent effects by simply multiplying the trace by the ratio of the autoconvolution and the frequency marginal, thus enforcing agreement of these two quantities. Remarkably, this correction procedure corrects, not only for all such known frequency-dependent effects, but for *unknown* effects, as well. In other words, even if one has not measured the spectral response of the diffraction grating or prism used for dispersion in the FROG device, any wavelength-dependence of this element will be compensated by this correction procedure. Of course, this procedure only works if no zeroes (or very low values) occur in the various wavelength-dependent responsivity, reflection, transmission, or efficiency curves. We will demonstrate the use of this procedure in Section V for a 12-fs pulse with a very large bandwidth of 150 nm.

Another experimental issue, particularly for multishot measurement of pulses on the order of 10 fs, is geometrical smearing of the delay due to the crossing angle within the SHG crystal. When two pulses cross at an angle, one pulse precedes the other on the right, and the other precedes the one on the left. This yields a range of delays across the beam simultaneously and is the effect that is utilized for single-shot autocorrelations and FROG measurements. In multishot measurements, on the other hand, when the delay is assumed to be fixed at a single value at any one time, this effect could smear out the temporal information in the FROG trace. This limitation also arises with traditional multishot background-free autocorrelation and in excite-probe measurements, and is well known.

We can exactly calculate the resulting trace shape and pulse width in the presence of this effect for a linearly chirped Gaussian-intensity pulse with Gaussian spatial profile, for which the SHG FROG trace is a product of Gaussians in delay and frequency in the absence of smearing. When geometrical smearing occurs, the measured SHG FROG trace is given by

$$\begin{aligned} I_{\mathrm{FROG}}^{\mathrm{SHG}}(\omega,\tau) &= \int_{-\infty}^{\infty}\left|\int_{-\infty}^{\infty} E\left[t+\left(\frac{x}{c}\right)\sin\left(\frac{\theta}{2}\right)\right]\right. \\ &\quad \left.\cdot\, E\left[t-\left(\frac{x}{c}\right)\sin\left(\frac{\theta}{2}\right)-\tau\right]\exp\left(-i\omega t\right)dt\right|^2 \\ &\quad \cdot\exp\left[-4\ln 2\cos^2\left(\frac{\theta}{2}\right)\frac{x^2}{d^2}\right]dx \end{aligned} \tag{7}$$

where x is the transverse spatial coordinate, d is the beam diameter, c is the speed of light in the medium, and θ is the beam crossing angle in the medium. Performing these integrals, we find that the trace remains the product of Gaussians in delay and in frequency. We find that no smearing occurs along the frequency axis, but the trace width along the delay axis increases. As a result, the SHG FROG trace continues to correspond exactly to a pulse, but it is a longer one. Thus, in the presence of this smearing, the FROG algorithm will precisely converge to a pulse, but the resulting pulse width, τ_p^{meas}, will be larger than the actual pulse width, τ_p, and is given by

$$(\tau_p^{\mathrm{meas}})^2 = \tau_p^2 + \delta t^2 \tag{8}$$

where

$$\delta t = \sqrt{2}\left(\frac{d}{c}\right)\tan\left(\frac{\theta}{2}\right). \tag{9}$$

When θ is small, $\delta t \approx \theta\, d/(\sqrt{2}c)$, and the speed of light in vacuum and the external angle can be used since the refractive index cancels out in this limit. For the 1.7° beam angle and 30-μm beam diameter used in this work, $\delta t = 2.1$ fs. For a 10-fs pulse, the measured pulse width will then be 10.2 fs, a 2% increase in width, which is not significant. This lengthening is identical in background-free autocorrelation. We conclude that, while one must keep this effect in mind when setting up apparatus, it plays a minimal role in SHG FROG as well as in autocorrelation.

It should be pointed out that the above effect can also smear out traces in other multishot versions of FROG (which use nonlinear effects other than SHG), but the resulting traces are unlikely to correspond to traces of actual pulses, as was the case above. This is because SHG FROG traces are necessarily symmetrical with respect to delay, and the traces of these other methods are not. For example, unlike SHG FROG, where the relative widths of the trace in the time and frequency directions indicate the chirp, it is instead the *slope* of the trace in other FROG methods that indicates the chirp. Thus, this effect should have even less an effect in these other versions of FROG.

It is this geometrical variation of the delay across the beam that makes single-shot measurements possible: in single-shot measurements, the beams are deliberately overlapped at a large angle, so that delay is varied across the nonlinear medium. The signal beam is then spatially resolved, yielding the signal pulse spectrum for this range of delays. Interestingly, a different geometrical smearing effect occurs in single-shot FROG measurements that do not use SHG [11], [20]. Because it does not occur in SHG FROG measurements, it is therefore not relevant to our measurements, but we mention it here for completeness. It results when the signal pulse does not propagate along the bisector between the two input beams and so is relevant to single-shot polarization-gate FROG measurements. In this case, the signal pulse also results from a range of delays, but, whereas the previous effect involved variation of the delay along the transverse direction, this effect involves variation of the delay in the longitudinal direction, that is, in the beam propagation direction. As a result, here, the smearing is now a function of the thickness of the nonlinear medium instead of the beam diameter. Fortunately, this effect has also been shown to be small, even for the shortest of pulses, provided that the medium is kept thin (<0.5 mm). Specifically, a temporal smearing of 10% of the gate pulse due to this effect results in a lengthening of the retrieved pulse of only about 1% [7]. And even if the temporal smearing of the gate pulse due to this effect is equal to the pulse length, the resulting lengthening of the retrieved pulse is less than 15% [7]. As a result, the lengthening of the retrieved pulses in such measurements can usually easily be reduced to below a few percent. And it can be corrected using a method developed by Tien *et al.* [20].

IV. Apparatus

Our SHG FROG apparatus is designed to minimize temporal and spectral aberrations in the measured ultrashort pulses. We use a 40%/40%, near-infrared, beamsplitter on a thin 5-μm pellicle substrate (National Photocolor), which has negligible dispersion. To avoid any possible bandwidth limitations of dielectric mirrors, we use protected silver mirrors throughout our setup. Instead of using a lens to focus the beams into the SHG crystal (which would add dispersion and temporal aberrations), we use a spherical mirror, with a 30-cm radius of curvature, to focus the pulses. As is shown in Fig. 4, this mirror is used near normal incidence to avoid astigmatism. For good second-harmonic conversion efficiency across our broad

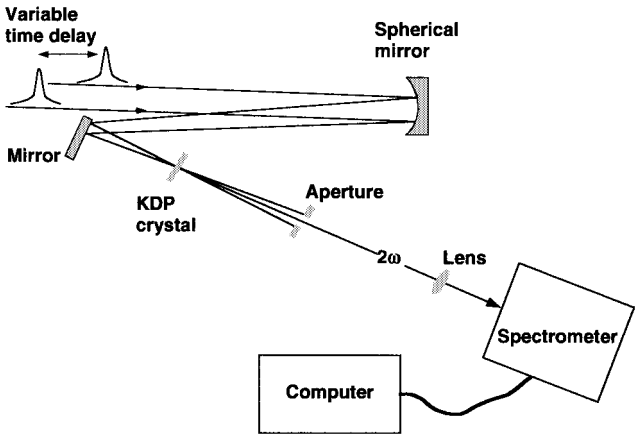

Fig. 4. Experimental setup for SHG FROG measurements of ~10-fs pulses.

bandwidths, we use a thin (0.4-μm thick) nonlinear poled polymer film of tricyanovinylaniline (PhTCV) for one set of measurements. We use a 60 $\pm$ 5-μm KDP crystal (Quantum Technology) for others. The spot size in the crystal is 30 μm, and we use a crossing angle of 1.7° to minimize temporal smearing. A 30-cm focal-length fused silica lens relays the second-harmonic signal into our spectrometer. After the SHG crystal, it is permissible to use a lens instead of a mirror, since dispersion after the frequency conversion process does not affect the spectral measurement.

Initially, our spectrometer consisted of a fused-silica prism, which dispersed the SHG light onto a CCD camera. Although this primitive spectrometer was inexpensive and had a relatively flat spectral response, calibration was difficult without a fixed entrance slit. Consequently, we now use a 0.15-m Acton Spectrapro 150 spectrometer, with a Santa Barbara Instruments ST6 CCD camera interfaced to a computer running LabVIEW. We take spectral data points separated by 0.41 nm. Because the quantum efficiency of the CCD camera varies significantly over the wavelength range of interest, the spectral response of our system was determined using the emission spectrum of a well characterized light bulb (Oriel 50W QTH). All spectral data are corrected in software for this nonuniform response. The time delay between the two arms is varied in increments of 1.5 fs using a microstepper motor (Melles Griot nanomover), which can provide subfemtosecond time-delay increments if necessary. All data are taken by continuously moving in one direction, to minimize the effects of backlash. Resulting arrays of points, typically 61 delays by 233 wavelengths, are converted to 128 $\times$ 128 arrays by zero-filling the delays (adding extra zeroes for large positive and negative delays beyond the scan range) and interpolating or taking a weighted average of the spectral values to yield a square array of points that obeys the discrete Fourier transform relation, that is, that the increment on each axis is the reciprocal of the range of the other axis. In addition, the data are corrected to be a plot of intensity versus delay and frequency, not wavelength, which is important because the Fourier transform relates time and frequency, not wavelength. This involves using a fixed frequency increment, not a fixed wavelength increment, between each data point, which requires a rescaling of the data (multiplying each point in the trace by $\lambda^2/2\pi c$, where λ is the wavelength) and is important for such broad frequency scans as this [11].

V. Measurements

The ultrashort pulses we measured were generated by a self-mode-locked Ti : Sapphire laser, described elsewhere [1]. Tuning of the pulse duration and pulse shape is possible by adjusting the intracavity dispersion by translation of one of the intracavity prisms. Our measurements focused on two different types of pulses: 1) a 13-fs near-transform-limited pulse and 2) a 12-fs pulse with a broad 150-nm-FWHM double-peaked spectrum. We measured the first using the thin-film nonlinear medium and the second using the 60-μm-thick KDP crystal.

Fig. 5(a) and (b) shows the experimental and retrieved FROG traces for the 13 fs pulse. We use density plots with overlaid contour plots to give maximal intuition in plots of these traces (although they tend to exaggerate small details in the wings of the trace at the expense of more important large-scale structure). We used a 128 $\times$ 128 grid and achieved an rms deviation between the experimental and retrieved traces, which we refer to as the "FROG error," of 0.0018, which is approximately equal to the noise in the data, and hence indicative of a good retrieval, given the data. Note that, by using contours at values as low as 2%, small deviations between the measured and retrieved traces are artificially emphasized, but it is nevertheless clear that the fit is visually very good, also. Indeed, deviations between measured and retrieved traces are on the order of the asymmetry in the measured trace, which is a good indicator of the random experimental error. The traces were cropped in these figures in order to show only their nonzero regions. Fig. 5(c) shows the corresponding retrieved temporal electric-field intensity and phase plotted versus time, and Fig. 5(d) shows the real electric-field waveform, carrier frequency included, of this extremely short pulse. (A future publication will provide an approach for computing error bars on the retrieved intensity and phase curves.) The small variation in the temporal phase over the pulse indicates that it is close to the transform limit. In fact, the shortest pulse supported by the spectral width, assuming a flat spectral phase, is 11 fs (FWHM). Because pulse shapes generated by the Ti : Sapphire laser in our regime of operation are not expected to be purely sech^2 or Gaussian [2], [21], observation of a nearly flat phase over the pulse is a much better experimental confirmation of a transform-limited pulse than simply measuring the width of an autocorrelation [3], [12], [14], [22].

In order to further check this measurement, we also measured the pulse spectrum independently and compared the spectrum autoconvolution with the FROG-trace frequency marginal. Fig. 6 shows the good agreement between the frequency marginal of the FROG trace and the autoconvolution of the spectrum. This confirms that there were no phase-matching or detection problems in this measurement.

For another confirmation of our ability to measure the pulse shape using FROG, we similarly measured a pulse, similar to

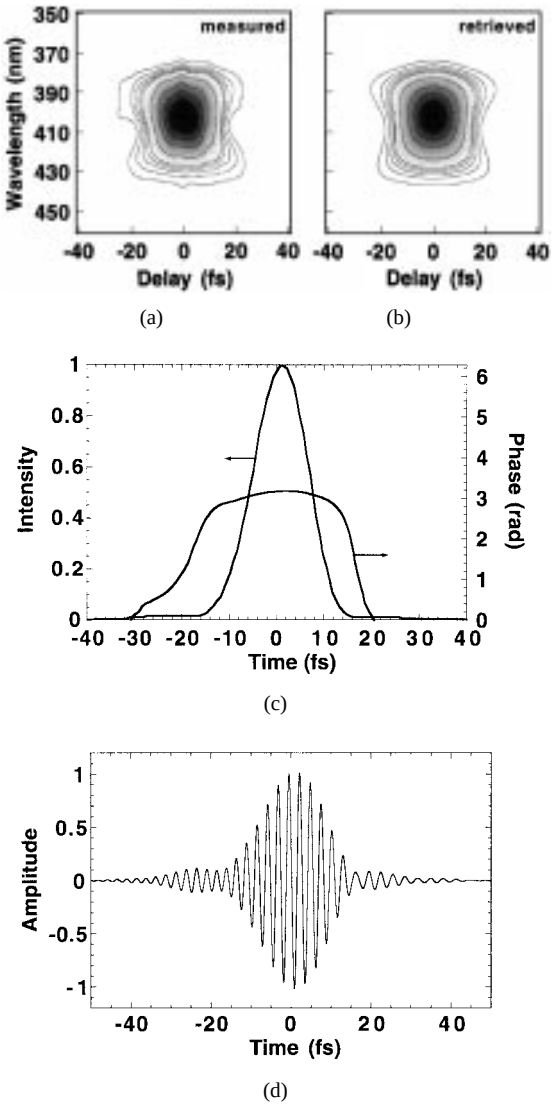

Fig. 5. (a) Experimentally measured SHG FROG trace of a 13 fs pulse, (b) retrieved FROG trace, (c) retrieved intensity (solid line) and phase (dashed line) of this pulse, and (d) retrieved real electric field of the pulse. In (a) and (b) (and in all other traces in this paper), the trace is shown as a density plot with overlaid contour lines at the values 2%, 4%, 6%, 8%, 10%, 20%, 40%, 60%, and 80%.

the one shown in Fig. 5, before and after passing through a 1-mm-thick fused silica window. Fig. 7 shows the intensity (circles) and phase (squares) measured after the window. As a comparison, we used the Sellmeier coefficients of fused silica to numerically add the dispersive effects of this material to the pulse measured before the window. The intensity and phase of this calculated chirped pulse are shown as the solid lines in Fig. 7. Although more appropriate techniques, such as spectral interferometry [23], exist for measuring small *relative* changes in phase, the good agreement in Fig. 8 shows FROG's ability to measure small changes in a pulse's intensity and phase, also. In addition, this verifies our measured pulse.

While measurement of the above 13-fs pulse proved to be relatively straightforward due to its near-transform-limited bandwidth of less than 100 nm and the use of a submicron nonlinear medium, the measurement of broader-band pulses in bulk crystals encounters phase-matching and potentially other

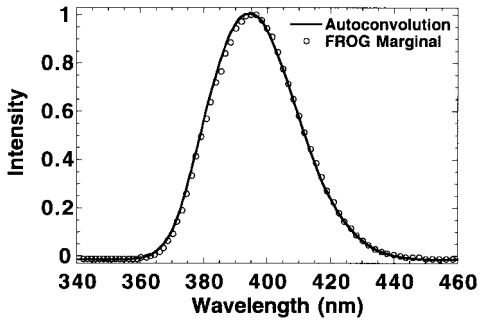

Fig. 6. Comparison of the autoconvolution (solid line) of the fundamental spectrum and the frequency marginal (circles) of the SHG FROG trace for a 13-fs pulse.

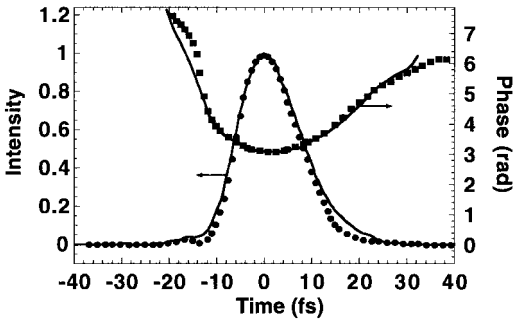

Fig. 7. Measured intensity (circles) and phase (squares) and calculated values (solid lines) of a pulse initially characterized to be nearly transform-limited that becomes slightly chirped after passing through a 1-mm-thick fused silica window.

wavelength-dependent-material problems, as discussed in Section III, and hence is correspondingly more difficult. This is, of course, the case for any pulse measurement technique. We will demonstrate, however, the previously described correction procedure in FROG and show that it can indeed correct for the apparatus inadequacies that are necessarily involved. The experimental SHG FROG trace of a 12-fs-duration, 150-nm-bandwidth pulse (whose generation is discussed in greater detail in the next section) is shown in Fig. 8(a). Fig. 8(b) shows the retrieved SHG FROG trace of this pulse, and Fig. 8(c) shows the retrieved intensity and phase in both domains. Note that convergence has occurred (the FROG error for this 128×128 trace is 0.002 73, approximately equal to the noise in the trace), and the retrieved SHG FROG trace agrees well with the experimental trace. Unfortunately, uniform phase-matching of the entire bandwidth of this pulse has not occurred, as shown by the comparison of the pulse autoconvolution with the FROG-trace frequency marginal in Fig. 9. Clearly, for the particular crystal angle used in the measurement, the crystal phase-matching efficiency is greater for the short wavelengths than for long ones. (Further evidence for this conclusion is that, for different SHG crystal angles, different spectral regions were underrepresented in the trace.) As a result, the retrieved pulse is suspect, despite the good convergence of the algorithm. Indeed, we have found that, while algorithm convergence is a very good indicator of a correct pulse measurement in other versions of FROG, convergence is usually, but not always, such an indicator in

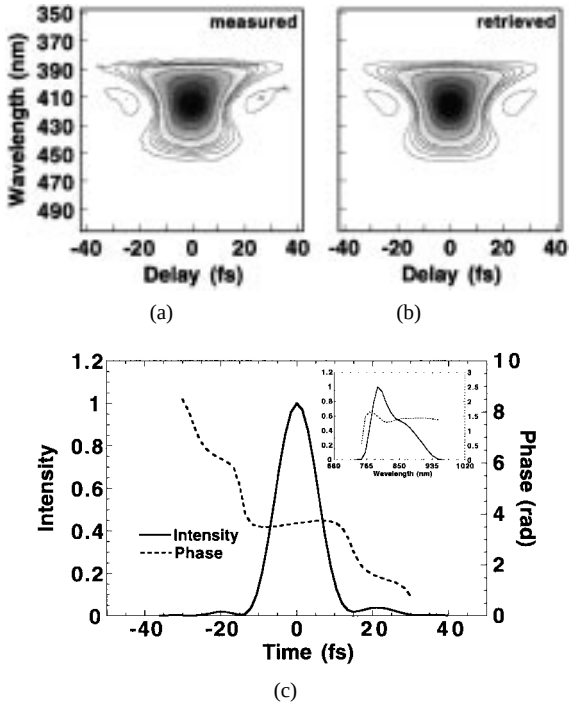

Fig. 8. FROG measurements using insufficient phase-matching bandwidth: (a) The experimentally measured SHG FROG trace for a 12-fs pulse with a double-peaked spectrum, (b) retrieved FROG trace, and (c) retrieved intensity and phase.

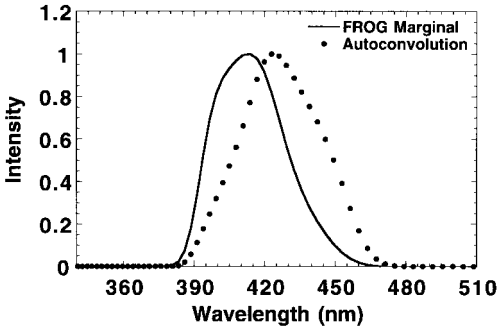

Fig. 9. Comparison of the autoconvolution and frequency marginal of the pulse whose trace is shown in the previous figure. Note the attenuated frequency marginal at long wavelengths compared to the autoconvolution of the spectrum, indicating poor phase-matching efficiency for those wavelengths.

SHG FROG, mainly due to the additional symmetry and time ambiguity of SHG FROG traces. Consequently, additional care must be used in SHG FROG measurements.

We can, however, as described in Section III, use the knowledge of the spectrum autoconvolution to correct the trace in order to force the frequency marginal to agree with it to compensate for the inadequate phase-matching bandwidth and potential wavelength-dependences of other components. Fig. 10(a) shows the corrected FROG trace using this procedure; Fig. 10(b) shows the retrieved FROG trace; and Fig. 10(c) shows the retrieved intensity and phase. The FROG error for this trace and its retrieved twin is 0.003 31, which is again approximately the experimental error (note that the error has increased slightly after using the correction procedure, because it has augmented regions of the trace that were formerly of low intensity, thus amplifying the noise

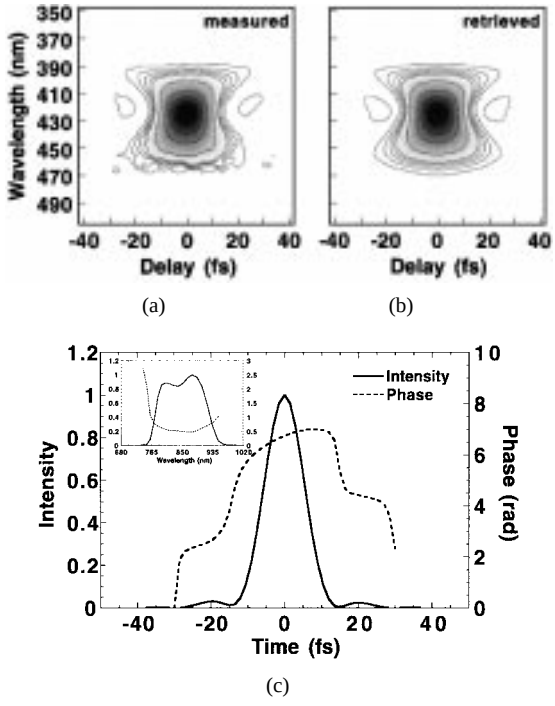

Fig. 10. Corrected FROG trace using the measured frequency marginal and spectrum autoconvolution: (a) The corrected experimental SHG FROG trace for a 12-fs pulse with a double peaked spectrum, (b) retrieved FROG trace, and (c) retrieved intensity and phase. Note the double-humped spectrum that was missing in the retrieved spectrum shown in Fig. 8.

somewhat, as can be seen in the corrected trace). Notice that the long-wavelength component of the often-seen double-peaked spectrum is much more evident in this retrieved pulse than in the previous retrieval using the uncorrected trace. Indeed, this measured spectrum agrees well with the independently measured pulse spectrum. As a result, this correction procedure has improved the pulse measurement considerably.

We note that the retrieved pulse is not of a sech^2 shape and that use of the usual 1.55 factor to obtain the pulse width from the autocorrelation width yields an 11-fs pulse width, not the actual 12-fs value. In general, we find that use of the 1.55 factor *under-predicts* the actual pulse width by about 10%, and that the Gaussian pulse shape, while also not exactly correct for these pulses, is a more accurate model for computing pulse shape from an autocorrelation. Of course, because no such correction procedure exists for autocorrelations, it is not clear what conclusions may be drawn from an autocorrelation in the presence of insufficient phase-matching bandwidth, as shown by Weiner over a decade ago [15].

We conclude that FROG's internal consistency check and its corresponding correction procedure is essential for the measurement of such broad-band—that is, extremely short—pulses.

VI. Comparison With Model

The ability of FROG to fully characterize ultrashort pulses has proved extremely useful in verifying the predictions of theoretical models of our laser [3], [12]–[14], [18]. Furthermore, agreement of theory and measurement also further

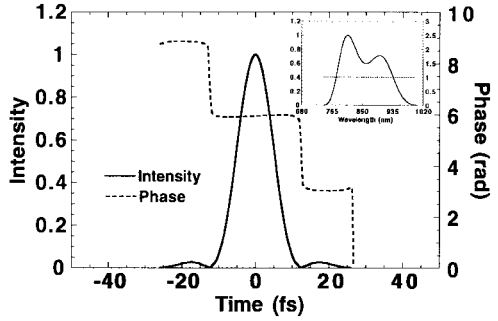

Fig. 11. The theoretically predicted (Kapteyn and co-workers) intensity and phase for the ∼10-fs pulse from a Ti:Sapphire oscillator dispersion-compensated up to, and including, third order.

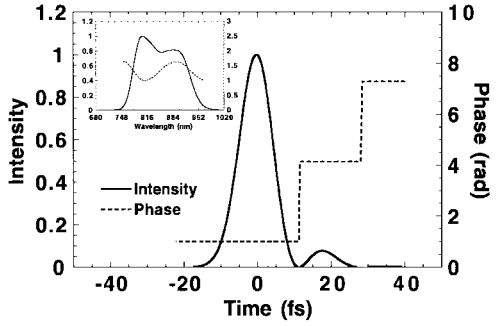

Fig. 12. The theoretically predicted (Harvey and co-workers) intensity and phase for the ∼10-fs pulse from a Ti:Sapphire oscillator limited by coherent ringing.

validates both the theory and the measurements. Numerical models of the Ti:Sapphire laser are necessary to describe the operation in the sub-20-fs regime, because analytical models can describe the operation only in a very limited regime of second-order dispersion-limited pulses, or at most fourth-order dispersion-limited pulses [21]. The Ti:Sapphire laser, however, can operate in more complicated intermediate regimes, with well-behaved, transform-limited, pulseshapes that are not necessarily sech^2 or Gaussian. Moreover, the slowly-varying envelope approximation cannot be assumed to be valid for pulse formation and nonlinear Kerr-lensing in these lasers, making numerical approaches [3], [12]–[14], [18] essential.

In order to generate the broad-bandwidth pulses with which to test our models, we operated at 850 nm, where both the second-and the third-order dispersion in the laser cavity were near-zero. Therefore, the femtosecond pulses were shaped and sustained by fourth-order dispersion. Fourth-order dispersion results in a large spectral region of near-zero group delay, which allows broader bandwidth operation than in the case of second-order dispersion. The output spectra from the laser were characteristically double-peaked, and were in excellent agreement with our model predictions (see Fig. 11), lending validity to our theory of higher order dispersion-limited pulse formation in Ti:Sapphire lasers [12], [18]. However, an alternative model of the double-peaked spectra suggested that it was the result of coherent ringing in the laser medium [24]. See Fig. 12. Although both theories could reproduce the observed pulse spectrum and autocorrelation (see Figs. 13 and 14), the

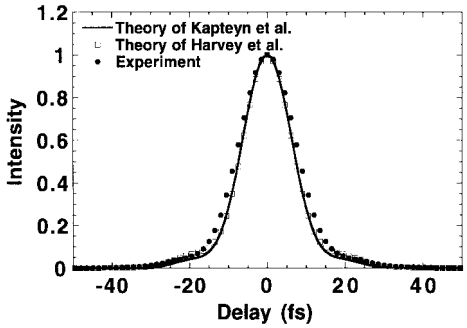

Fig. 13. Measured and theoretically predicted autocorrelations for the ∼10-fs pulse from a Ti:Sapphire oscillator. Note that, although the measured pulse is slightly longer, all autocorrelations are similar in shape.

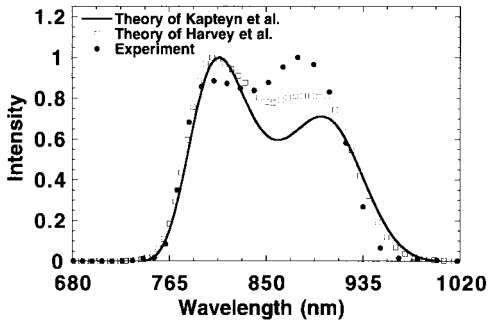

Fig. 14. Measured and theoretically predicted spectra for the ∼10-fs pulse from a Ti:Sapphire oscillator. Note that all spectra display the characteristic double-humped shape. (The relative heights of the two spectral peaks vary from measurement to measurement and so should not be considered able to distinguish between the theories.)

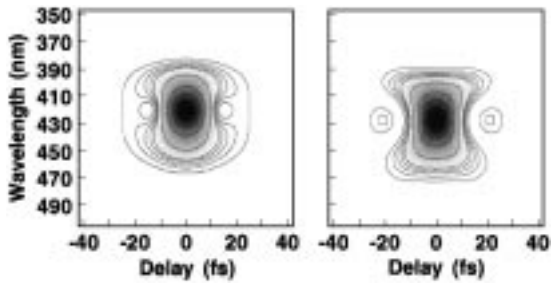

(a) (b)

Fig. 15. Theoretically predicted FROG traces for the ∼10-fs pulse from a Ti:Sapphire oscillator. Note that the trace predicted by Kapteyn and co-workers (right) agrees much better with the measured FROG trace (shown in Fig. 10) than that of Harvey and co-workers (left).

two theories predict very different pulse shapes. In particular, note the symmetrical satellite pulses in the intensity of our theory and the satellite pulses on only the trailing side of the intensity of the alternate theory. Only a technique like FROG can distinguish between the two different theories. Fig. 15 shows the SHG FROG traces for the two theoretically predicted pulses. Fig. 10 shows the experimentally measured FROG trace, which agrees much better with that predicted by our high-order dispersion-limited theory. In addition, the intensity versus time of the pulse also agrees with our theory [3], [12]–[14].

Given the detailed and rigorous tests that FROG allows us to perform on our data and theoretical models, we can proceed

with confidence to predict the shortest duration pulses that can be generated in Ti:Sapphire, given an ideal amount of dispersion. Our model predicts that pulses as short as 5 fs can be produced from a laser with optimal fourth-order dispersion compensation. Proper design of intracavity dispersion is a technological, rather than fundamental, problem, and thus we can expect to generate extremely short pulses directly out of a laser in the future.

VII. Conclusion

SHG FROG measurements of pulses on the order of 10 fs provide a powerful diagnostic of ultrashort-pulse formation and propagation. The self-consistent checks and resulting correction procedure present in the FROG technique guarantee that the measured pulsewidths are accurate and thus make FROG vastly superior to traditional techniques, which are prone to experimental errors that cannot be verified. Future effort will be devoted to the question of the breakdown of the slowly varying envelope approximation in the measurement process itself, which is beyond the scope of this paper but certainly must be resolved before even shorter pulses can be measured—whether by FROG or any other method.

References

[1] J. Zhou, G. Taft, C. P. Huang, M. M. Murnane, H. C. Kapteyn, and I. Christov, "Pulse evolution in a broad bandwidth Ti:sapphire laser," *Opt. Lett.*, vol. 19, no. 15, pp. 1149–1151, 1994.

[2] L. Xu, C. Spielmann, F. Krausz, and R. Szipocs, "Ultrabroadband ring oscillator for sub-10-fs pulse generation" *Opt. Lett.*, vol. 21, no. 16, pp. 1259–1261, 1996.

[3] I. P. Christov, V. Stoev, M. Murnane, and H. Kapteyn, "Sub-10 fs operation of Kerr-lens modelocked lasers," *Opt. Lett.*, vol. 21, pp. 1493–1495, 1996.

[4] M. Nisoli, S. D. Silvestri, and O. Svelto, "Generation of high energy 10 fs pulses by a new pulse compression technique," *Appl. Phys. Lett.*, vol. 68, p. 2793, 1996.

[5] K. L. Sala, G. A. Kenney-Wallace, and G. E. Hall, "Cw autocorrelation measurements of picosecond laser pulses," *IEEE J. Quantum Electron.*, vol. QE-16, pp. 990–996, Sept. 1980.

[6] D. J. Kane and R. Trebino, "Characterization of arbitrary femtosecond pulses using frequency resolved optical gating," *IEEE J. Quantum Electron.*, vol. 29, pp. 571–579, Feb. 1993.

[7] K. W. DeLong, R. Trebino, J. Hunter, and W. E. White, "Frequency-resolved optical gating with the use of second-harmonic generation," *J. Opt. Soc. Amer. B*, vol. 11, no. 11, pp. 2206–2215, 1994.

[8] K. W. DeLong, R. Trebino, and D. J. Kane, "Comparison of ultrashort-pulse frequency-resolved-optical-gating traces for three common beam geometries," *J. Opt. Soc. Amer. B*, vol. 11, no. 9, pp. 1595–1608, 1994.

[9] K. W. DeLong, D. N. Fittinghoff, R. Trebino, B. Kohler, and K. Wilson, "Pulse retrieval in frequency-resolved optical gating based on the method of generalized projections," *Opt. Lett.*, vol. 19, no. 24, pp. 2152–2154, 1994.

[10] K. W. DeLong, D. N. Fittinghoff, R. Trebino, and C. L. Ladera, "Noise sensitivity in frequency-resolved-optical-gating measurements of ultrashort pulses," *J. Opt. Soc. Amer. B*, vol. 12, no. 10, p. 1955, 1995.

[11] K. W. DeLong, D. N. Fittinghoff, and R. Trebino, "Practical issues in ultrashort-laser-pulse measurement using frequency-resolved optical gating," *IEEE J. Quantum Electron.*, vol. 32, pp. 1253–1264, July 1996.

[12] I. P. Christov, M. M. Murnane, H. C. Kapteyn, J. P. Zhou, and C. P. Huang, "Fourth-order dispersion limited solitary pulses," *Opt. Lett.*, vol. 19, no. 18, pp. 1465–1467, 1994.

[13] I. P. Christov, H. C. Kapteyn, M. M. Murnane, C. P. Huang, and J. P. Zhou, "Space-time focusing of femtosecond pulses in Ti:sapphire," *Opt. Lett.*, vol. 20, no. 3, pp. 309–311, 1995.

[14] I. P. Christov, V. Stoev, M. Murnane, and H. Kapteyn, "Mode-locking with a compensated space-time astigmatism," *Opt. Lett.*, vol. 20, no. 20, pp. 2111–2113, 1995.

[15] A. M. Weiner, "Effect of group velocity mismatch on the measurement of ultrashort optical pulses via second harmonic generation," *IEEE J. Quantum Electron.*, vol. QE-19, pp. 1276–1283, Aug. 1983.

[16] R. Fischer and C. Rempel, "Deformation and reconstruction of auto-correlation functions," in *Proc. Eighth Vavilov Conf. Nonlinear Optics*, 1985, p. 198.

[17] T. Mindl, P. Hefferle, S. Schneider, and F. Dorr, "Characterization of a train of subpicosecond laser pulses by fringe-resolved autocorrelation measurements," *Appl. Phys. B*, vol. 31, pp. 201–207, 1983.

[18] G. Taft, A. Rundquist, M. M. Murnane, H. C. Kapteyn, K. DeLong, R. Trebino, and I. P. Christov, "Ultrafast optical waveform measurements using frequency-resolved optical gating," *Opt. Lett.*, vol. 20, no. 7, pp. 743–745, 1995.

[19] D. R. Yankelevich, A. Knoesen, G. Taft, M. M. Murnane, H. C. Kapteyn, and R. J. Twieg, "Molecular engineering of polymer films for amplitude and phase measurements of Ti:sapphire femtosecond pulses," *Opt. Lett.*, vol. 21, no. 18, pp. 1487–1489, 1996.

[20] A.-C. Tien, S. Kane, J. Squier, B. Kohler, and K. Wilson, "Geometrical distortions and correction algorithm in single-shot pulse measurements: Application to frequency-resolved optical gating," *J. Opt. Soc. Amer. B*, vol. 13, no. 6, pp. 1160–1165, 1996.

[21] I. P. Christov, H. C. Kapteyn, and M. M. Murnane, "Comment on 'sub 10 fs, mirror-dispersion controlled Ti : sapphire laser' by A. Stingl *et al.*," *Opt. Lett.*, vol. 20, p. 602, 1995, submitted 1996.

[22] M. Piche, J. F. Cormier, and X. Zhu, "Bright optical soliton in the presence of fourth-order dispersion," *Opt. Lett.*, vol. 21, no. 12, p. 845, 1996.

[23] D. N. Fittinghoff, J. L. Bowie, J. N. Sweetser, R. T. Jennings, M. A. Krumbügel, K. W. DeLong, R. Trebino, and I. A. Walmsley, "Measurement of ultraweak ultrashort laser pulses," *Opt. Lett.*, vol. 21, no. 12, pp. 884–886, 1996.

[24] J. D. Harvey, J. M. Dudley, P. F. Curley, C. Spielmann, and F. Krausz, "Coherent effects in a self-modelocked Ti:sapphire laser," *Opt. Lett.*, vol. 19, no. 13, p. 972, 1994.

Greg Taft received the M.S. degree in physics from Washington State University in 1994 and the B.A. degree in physics from Saint John's University in Collegeville, MN, in 1992, and will defend his Ph.D. dissertation in physics from Washington State University in May of 1997.

He has investigated the limiting physics of ultrashort pulse generation and measurement, working as a graduate student in the group of Profs. H. Kapteyn and M. Murnane at the Center for Ultrafast Optics at the University of Michigan.

Andy Rundquist received the M.S. degree in physics from Washington State University in 1995, and the B.A. degree from St. John's University, Collegeville, MN, in 1993, and is currently seeking the Ph.D. degree in physics from Washington State University.

He is doing research on ultrashort pulse characterization and application to high-field atomic interactions at the Center for Ultrafast Optical Science at the University of Michigan. His advisors are Profs. M. Murnane and H. Kapteyn.

Margaret M. Murnane (M'92) received the Ph.D. degree in physics from the University of California, Berkeley, CA, in 1989, where she worked on generating ultrafast X-ray pulses from high-density laser-produced plasmas.

She joined the faculty at Washington State University in 1990. In 1996, she moved to the University of Michigan and the Department of Electrical Engineering and Computer Science. She is also a member of the Center for Ultrafast Optical Science, a National Science Foundation Science and Technology Center. Her work has been part of a recent revolution in ultrafast phenomena. Visible and X-ray pulses, as short as three optical cycles in duration, can now be simply and reliably generated and powerful new techniques can obtain accurate information on the exact shape of ultrashort pulses, which are revolutionizing the way we think about and use light to manipulate matter.

Prof. Murname's honors include the American Physical Society Simon Ramo Award, an Alfred P. Sloan Foundation Fellowship, a National Science Foundation Presidential Faculty Fellowship, and the 1997 Maria Goeppert-Mayer Award of the American Physical Society. Prof. Murnane is member of the American Physical Society, the Optical Society of America, and the Association for Women in Science.

Ivan P. Christov, photograph and biography not available at the time of publication.

Henry C. Kapteyn received the Ph.D. degree in physics from the University of California, Berkeley, CA, in 1989, in the field of X-ray and short-wavelength laser physics.

He has been at the University of Michigan's Center for Ultrafast Optical Science (CUOS) since January 1996. In 1990, he joined the Physics Department at Washington State University as an Assistant Professor. His work at WSU, done in collaboration with Prof. M. Murnane, resulted in the development of a new generation of lasers which make it straightforward to produce light pulse of less than ten femtoseconds duration. In 1996, he joined the Electrical Engineering Department at the University of Michigan. At CUOS, he is applying this laser technology to the generation and application of ultrashort-pulse X-ray and VUV light.

Prof. Kapteyn is the recipient of a National Science Foundation Young Investigator Award in 1992, the Optical Society of America's 1993 Adolph Lomb Medal, and an Alfred P. Sloan Foundation Fellowship.

Kenneth W. DeLong was born in Allentown, PA, in 1962. He received the B.S. degree in physics from Penn State University, University Park, PA, in 1984, and the Ph.D. degree in optical sciences in 1990 from the University of Arizona, Tucson.

From 1990 to 1992, he was with NTT Basic Research Laboratories in Tokyo, Japan, working on femtosecond spectroscopy of semiconductor microcrystals, soliton interactions, and dynamics of discrete nonlinear equations. While at Sandia National Laboratory, Livermore, CA, he was engaged in the characterization of ultrashort laser pulses. Currently, he is with Lawrence Livermore Laboratories, Livermore, CA.

David N. Fittinghoff received the B.S. degree in physics and the M.S. and Ph.D. degrees from the University of California at Davis, in 1985, 1990, and 1993, respectively.

After receiving the B.S. degree, he participated in research on the generation of high-power microwaves at Physics International. After receiving the Ph.D. degree, he joined the group of Dr. Rick Trebino at Sandia National Laboratories' Compustion Research Facility, Livermore, CA, working in the fields of ultrashort pulse lasers and their applications, ultrashort pulse measurements, optical inverse scattering, and neural networks. His current appointment is with the University of California at San Diego in the group of Prof. Kent Wilson.

Marco A. Krumbügel received the Diplom in Physics and the Dr. rer. nat. degree from the Technical University of Berlin, Berlin, Germany, in 1990 and 1993, respectively.

His thesis research involved numerical simulations and interferometric microwave measurements of the diffraction near fields behind phase objects. Since 1995 he has held a Feodor Lynen Fellowship of the Alexander von Humboldt Foundation, working in collaboration with Dr. Rick Trebino from Sandia National Laboratories and Prof. Anthony E. Siegman from Stanford University to retrieve ultrashort laser pulses using Frequency-Resolved Optical Gating and an artificial neural network.

Dr. Krumbügel is member of the Optical Society of America, the Deutsche Physikalische Gesellschaft, and the Deutsche Gesellschaft für angewandte Optik.

John N. Sweetser received the B.S. degree in applied and engineering physics and the M.Eng. degree in electrical engineering from Cornell University, Ithaca, NY, in 1984 and 1986, respectively, and the Ph.D. degree in optics from the University of Rochester, Rochester, NY, in 1994.

His thesis research involved the study of coherent effects in the propagation of ultrashort laser pulses in resonant molecular systems and the development of a novel femtosecond laser amplifier. He is currently with Sandia National Laboratories, where he is developing techniques for linear and nonlinear optical spectroscopy for gas-phase diagnostics. His other interests include ultrashort pulse measurement and applications and optical switching.

Rick Trebino was born in Boston, MA, on January 18, 1954. He received the B.A. degree from Harvard University, Cambridge, MA, in 1977, and the Ph.D. degree from Stanford University, Stanford, CA, in 1983, where he developed a technique for measuring ultrafast events by inducing moving gratings.

In 1986, he joined Sandia National Laboratories, Livermore, CA, where he has studied higher-order wave-mixing effects, nonlinear optical perturbation theory using Feynman diagrams, and the measurement and use of ultrashort laser pulses.